The Phase Shift of an Ultrasonic Pulse at an Oil Layer and Determination of Film Thickness

T. Reddyhoff[1], S. Kasolang[1], R.S.Dwyer-Joyce[1], B.W.Drinkwater[2].

[1]Department of Mechanical Engineering,
Mappin Street, University of Sheffield, Sheffield S1 3JD, UK

[2]Department of Mechanical Engineering,
University Walk, University of Bristol, Bristol BS8 1TR, UK

Keywords

Oil film thickness measurement, ultrasound, phase difference, phase shift, ultrasonic reflection

Abstract

An ultrasonic pulse incident on a lubricating oil film in a machine element will be partially reflected and partially transmitted. The proportion of the wave amplitude reflected, termed the reflection coefficient, depends on the film thickness and the acoustic properties of the oil. When the appropriate ultrasonic frequency is used, the magnitude of the reflection coefficient can be used to determine the oil film thickness. The reflected wave, however, has both a real and an imaginary component, and both the amplitude and phase are functions of the film thickness. The phase of the reflected wave will be shifted from that of the incident wave when it is reflected. In the present study this phase shift is explored as the film changes and is evaluated as an alternative means to measure oil film thickness.

A quasi-static theoretical model of the reflection response from an oil film has developed. The model relates the phase shift to the wave frequency and the film properties. Measurements of reflection coefficient from a static model oil film and also from a rotating journal bearing have been recorded. These have been used to determine the oil film thickness using both amplitude and phase shift methods. In both cases, the results agree closely with independent assessments of the oil film thickness. The model of ultrasonic reflection is further extended to incorporate mass and damping terms. Experiments show that both the mass and the internal damping of the oil films tested in this work has a negligible effect on ultrasonic reflection.

A potentially very useful application of the simultaneous measurement of reflection coefficient amplitude and phase is that it the data can be used to negate the need for a reference. The theoretical relationship between phase and amplitude is fitted to the data. An extrapolation is performed to determine values of amplitude and phase for an infinitely thick layer. This is equivalent to the reference signal determined from measuring the reflection coefficient directly, but importantly does not require the materials to be separated. This provides a simple and effective means of continuously calibrating the film measurement approach.

Introduction

The thickness of the oil film in tribological components is a key parameter. If the film is too thin then surface contact can occur resulting in high friction and wear. If the film is too thick energy is expended needlessly in overcoming churning loses. The film is usually so thin that it is small compared to elastic distortions of the bearing elements. For this reason, measurement of the bulk separation of the bearing components is not usually sensitive enough to deduce the oil film thickness. Electrical resistance and capacitance have proved useful methods, as have optical methods. However, both these approaches require modifications to the bearing machinery that frequently preclude their application outside of the laboratory [1-5].

One method that shows potential for non-invasive oil film measurement is the use of ultrasonic reflection. An ultrasonic transducer can be coupled to the outside of a bearing and a wave transmitted through the bearing shell. The wave is partially reflected when it strikes an oil film. The proportion of the wave reflected, known as the reflection coefficient, depends on, amongst other parameters, the thickness of the oil film.

The response of a thin intermediate layer between two solid bodies to an ultrasonic wave can be conveniently determined using a quasi-static spring model. If the ultrasound is normally incident on a thin layer the magnitude of the reflection coefficient is given by [6]:

$$|R| = \sqrt{\frac{(\omega z_1 z_2)^2 + K^2 (z_1 - z_2)^2}{(\omega z_1 z_2)^2 + K^2 (z_1 + z_2)^2}} \tag{1}$$

where ω is the angular frequency of the ultrasonic wave and z is the acoustic impedance (the product of the wave speed, c and the density ρ) and the subscripts 1 and 2 refer to the materials either side of the layer. The term K is the stiffness of the interfacial layer, and represents the compression of the layer with changing contact pressure. In the context of such thin layers (thin with respect to the ultrasonic wavelength), the reflection is dominated by the stiffness of the layer and it is assumed that mass and damping have insignificant contribution to the coefficient of reflection.

For the purposes of the analysis, the layer can be a film of homogenous material (liquid or solid) between two solid bodies, or a region of reduced stiffness, for example a rough surface contact. This spring model method has been successfully used to study adhesive bonds [6, 7, 8], cracks under compressive loading [9, 10] and rough surface contact phenomenon [11, 12, 13]. In the latter case measurements of phase shift have also been used to determine additional features of the rough surface contact [14, 15].

Oil films in engineering bearing components are typically very thin (and acoustically dissimilar from the bearing materials) and the spring model approach provides a suitable method for interpreting their ultrasonic response. In Dwyer-Joyce et al. [16] the approach was evaluated for hydrodynamic and elastohydrodynamic oil film thickness measurement. The stiffness of the oil film is a function of its bulk modulus, B and film thickness, h according to:

$$K = \frac{B}{h} \tag{2}$$

Or in terms of the oil's acoustic properties:

$$K = \frac{\rho c^2}{h} \tag{3}$$

where ρ is the oil density and c is the speed of sound through the oil. Combining (1) and (3) gives a relationship between reflection coefficient and liquid film thickness. This has subsequently been used to measure the oil film in rolling element bearings [17], hydrodynamic journal bearings [18], piston ring liner contacts [19], and thrust pad bearings [20]. All the ultrasonic studies outlined above rely on the measurement of reflection coefficient i.e. the fraction of incident wave reflected. In order to obtain this proportion, the reflection from the interface is compared to the reflection from a material/air interface where the complete reflection occurs. Practically this requires the surfaces on either side of the interface to be separated and a reference measurement taken against which subsequent reflections are compared. In a journal bearing film monitoring for instance this entails removal of the journal from the bush.

This reference taking procedure is not ideal, as it requires machinery stopped and components disassembled before film thickness can be measured. The reference can then degrade with time (and potentially is subject to temperature changes). Measuring new references by disassembly is at least costly and under certain circumstances makes oil film monitoring unfeasible. The benefits of film monitoring have been established. Two solutions to this problem exist. Firstly measuring layer thickness by some means other than using spring stiffness (for example the use of a time of flight or resonance method, as described in [16], for thicker films) or secondly, measuring reflection coefficient without taking a reference.

As the reflection coefficient contains both magnitude and phase information it is common to describe it using complex number notation. However, in previous work, only the variation of reflection coefficient amplitude has been studied and used to determine the oil film thickness. The phase however also changes and may be useful in providing an alternative method for determining oil film properties. Amplitude based methods are commonly subject to measurement errors; potentially a phase based could be less prone to noise.

In this paper the spring model has been elaborated to relate the oil film properties to the phase shift of the reflected ultrasonic wave. A series of ultrasonic reflection experiments from a static oil film and an oil film in a rotating journal bearing have been performed. The model has then been used to interpret these reflections and hence determine the oil film thickness by both phase and amplitude methods. The deduced film thickness measurements have been compared with measurements by independent means. It is also possible to use this model to relate amplitude and phase by simple expression. Curve fitting measured data to this expression provides a useful way of providing an independent reference signal.

Ultrasonic Reflection at an Oil Film

Consider the three-layered system as shown in figure 1, each layer having an associated speed of sound c_i and acoustic impedance z_i.

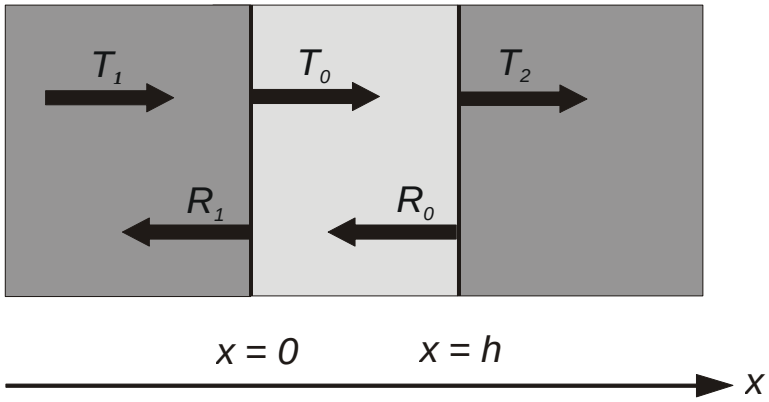

Figure 1. Schematic diagram of an ultrasonic wave travelling through a three-layer system.

In medium 1 an incident acoustic displacement wave of unit amplitude propagating in the direction x can be represented by: $u_i = e^{i\omega(t-x/c_i)}$

At the interface between media 1 and 0, part of the wave is transmitted into medium 0, while part is reflected back into medium 1. The fraction of the wave transmitted through an interface (the transmission coefficient) is denoted by *T*, whilst that reflected back (the reflection coefficient) is denoted by *R*. The total displacements in media 1, 0, and 2 are therefore given by:

$$u_1(x) = e^{-i\omega x/c_1} + R_1 e^{i\omega x/c_1} \tag{4}$$

$$u_0(x) = T_0 e^{-i\omega x/c_0} + R_0 e^{i\omega x/c_0} \tag{5}$$

$$u_2(x) = T_2 e^{-i\omega x/c_2} \tag{6}$$

where the term $e^{i\omega t}$ has been omitted for simplicity. Differentiating with respect to x and applying the stress strain relationship gives the stress in each medium, σ:

$$\sigma_1(x) = -i\omega \frac{E_1}{c_1}\left(e^{-i\omega x/c_1} - R_1 e^{i\omega x/c_1}\right) \tag{7}$$

$$\sigma_0(x) = -i\omega \frac{E_0}{c_0}\left(T_0 e^{-i\omega x/c_0} - R_0 e^{i\omega x/c_0}\right) \tag{8}$$

$$\sigma_2(x) = -i\omega \frac{E_2}{c_2} T_2 e^{-i\omega x/c_2} \tag{9}$$

Where E_i is the Young's modulus of medium *i*. The modulus can be replaced by the acoustic impedance ($E_i = z_i c_i$) so equations (7) to (9) become:

$$\sigma_1(x) = -i\omega z_1\left(e^{-i\omega x/c_1} - R_1 e^{i\omega x/c_1}\right) \tag{10}$$

$$\sigma_0(x) = -i\omega z_0\left(T_0 e^{-i\omega x/c_0} - R_0 e^{i\omega x/c_0}\right) \tag{11}$$

$$\sigma_2(x) = -i\omega z_2 T_2 e^{-i\omega x/c_2} \tag{12}$$

Assuming the interfaces 1-0 and 0-2 are perfectly bonded and have negligible mass, then the boundary conditions of continuous stress and displacement are:

$$u_1(0) = u_0(0), \quad u_0(h) = u_2(h) \tag{13}$$

$$\sigma_1(0)=\sigma_0(0),\ \ \sigma_0(h)=\sigma_2(h) \tag{14}$$

Combining these relationships gives:

$$R_1=\frac{e^{-i\omega h/c_0}(z_1+z_0)(z_0-z_2)-e^{i\omega h/c_0}(z_0-z_1)(z_0+z_2)}{e^{-i\omega h/c_0}(z_0-z_1)(z_2-z_0)+e^{i\omega h/c_0}(z_1+z_0)(z_0+z_2)} \tag{15}$$

which is the exact analytical solution for the reflection coefficient from a three layered system. This will now be simplified for the special case where the intermediate layer is thin and of lower acoustic impedance than the surrounding media (which is typical for an oil film).

The exponential terms can be written as a Taylor expansion:

$$e^{i\omega h/c_0}=1+i\omega h/c_0+\frac{(i\omega h/c_0)^2}{2!}+\frac{(i\omega h/c_0)^3}{3!}+... \tag{16}$$

$$e^{-i\omega h/c_0}=1-i\omega h/c_0+\frac{(-i\omega h/c_0)^2}{2!}+\frac{(-i\omega h/c_0)^3}{3!}+... \tag{17}$$

which can then be substituted into (15) to give:

$$R=\frac{2z_0(z_1-z_2)+2A(z_1z_2-z_0^2)+A^2z_0(z_1-z_2)+\frac{A^3}{3}(z_1z_2-z_0^2)+...}{2z_0(z_1+z_2)+2A(z_1z_2+z_0^2)+A^2z_0(z_1+z_2)+\frac{A^3}{3}(z_1z_2+z_0^2)+...} \tag{18}$$

where $A=i\omega h/c_0$. If the intermediate layer (medium 0) is thin compared with the ultrasonic wavelength, then $\omega h/c_0\to 0$ and so only the first order terms in the Taylor series expansion are considered:

$$R=\frac{z_0(z_1-z_2)+i\omega h/c_0(z_1z_2-z_0^2)}{z_0(z_1+z_2)+i\omega h/c_0(z_1z_2+z_0^2)} \tag{19}$$

If z_0 is small compared to z_1 and z_2, then (19) reduces to:

$$R=\frac{(z_1-z_2)+i\omega h/z_0c_0(z_1z_2)}{(z_1+z_2)+i\omega h/z_0c_0(z_1z_2)} \tag{20}$$

If we substitute $z=\rho c$, equation (20) becomes

$$R=\frac{(z_1-z_2)+i\omega h/\rho_0c_0^2(z_1z_2)}{(z_1+z_2)+i\omega h/\rho_0c_0^2(z_1z_2)} \tag{21}$$

Combining equation (21) with equation (3) gives the reflection coefficient in terms of layer stiffness *K*.

$$R=\frac{(z_1-z_2)+i\omega/K(z_1z_2)}{(z_1+z_2)+i\omega/K(z_1z_2)} \tag{22}$$

Equation (22) shows the reflection coefficient as a complex quantity containing amplitude and phase information. Here reflection coefficient has been derived in terms of displacement. It is equally valid to derive the reflection coefficient in terms of pressure. In the analysis that follows assumes a displacement derived reflection coefficient.

If the amplitude of the reflection coefficient is determined from equation (20) and equation (3) is used to substitute for oil film thickness then the basic amplitude spring model, equation (1), is obtained.

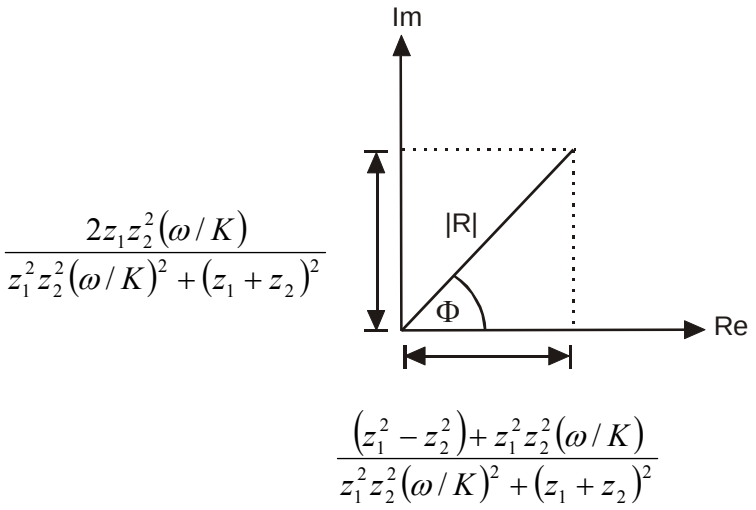

Figure 2. Representation the reflection coefficient from an intermediate layer as a complex quantity on an Argand diagram.

From figure 2 it can be seen that the phase shift, Φ_R associated with the reflection coefficient (i.e. the phase difference between the incident and reflected waves) is obtained by trigonometry from equation 21.

$$\Phi_R = \arctan\left(\frac{2\omega z_1 z_2^2 / K}{(z_1 - z_2) + \omega^2 (z_1 z_2 / K)^2}\right) \tag{23}$$

The phase difference, between an incident and reflected wave, thus varies from 0 for a thick film ($K \to 0$), to $\pi/2$ for a thin film ($K \to \infty$) as shown schematically in figure 3. It should be noted that if the second medium were acoustically less dense than the first ($z_2 < z_1$), then the phase difference for a vanishingly thin film would be π.

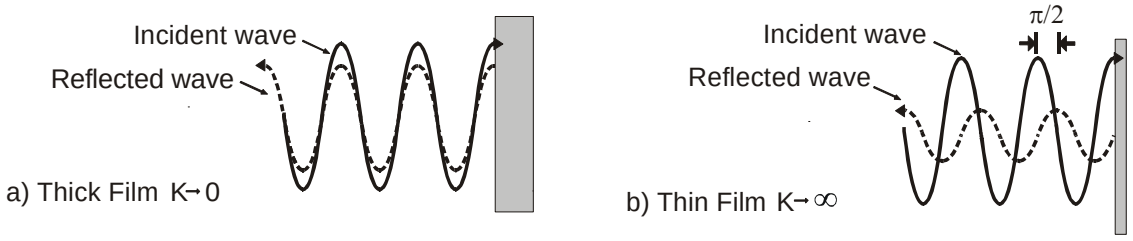

Figure 3. Schematic representation of the phase difference and amplitude reduction between an incident and reflected wave at thick and thin oil films.

In the experimental work no outgoing incident signals are recorded; only signals reflected from the interface. The reflection coefficient is obtained by first recording a reflection at a solid to air boundary. This is equivalent to the incident signal and is used as a reference. All subsequent reflections are compared to this reference to give the reflection coefficient. Reflection coefficient amplitude and phase difference are thus determined relative to this reference signal.

The film thickness can then be expressed in terms of reflection coefficient *amplitude* by combining (1) and (3):

$$h = \frac{\rho c^2}{\omega z_1 z_2} \sqrt{\frac{R^2 (z_1 + z_2)^2 - (z_1 - z_2)^2}{1 - R^2}} \tag{24}$$

or in terms of the *phase difference*, between reflected and incident waves, by combining (23) and (3):

$$h = \frac{\rho c^2 (\tan \Phi_R)(z_1^2 - z_2^2)}{\omega z_1 z_2^2 \pm \sqrt{(\omega z_1 z_2^2)^2 - (\tan \Phi_R)^2 (z_1^2 - z_2^2)(\omega z_1 z_2)^2}} \tag{25}$$

If accoustic impedances either side of the interface are assumed to be equal, and (24) is equated to (25) a simple result is obtained:

$$|R| = \cos \Phi_R \tag{26}$$

Figure 4 shows a plot of equation (23) for various thickness mineral oil films between steel surfaces. The predicted phase difference depends on the frequency of the incident ultrasonic wave. In principle therefore, the phase difference at any frequency could be used to determine the stiffness and hence the thickness of the oil film in equation (25). In practice however, the measured phase difference should be distinguishable from background noise, and a suitable region of the graph must be used. For example, an oil film of 5 μm will show cause a negligible phase change in a wave of frequency greater than say 30 MHz. However, an oil film of thickness 0.5 μm will cause a phase change of ~π/3 in a 40 MHz incident wave.

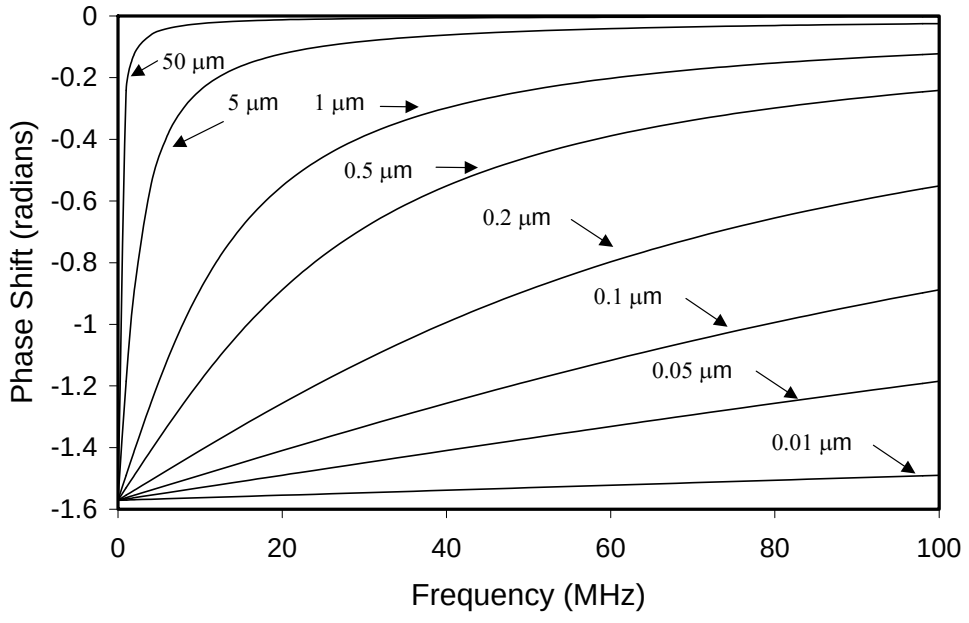

Figure 4. Variation of phase difference between incident and reflected waves with ultrasonic frequency, according to equation (23). The different curves are for different thickness oil films between steel surfaces.

Measurement Apparatus

A piezoelectric transducer was located such that it could send and receive pulses perpendicular to the oil film. The transducer was coupled to the specimen either by using a water gel based couplant or with a permanent adhesive bond. In this work commercial longitudinal planar transducers were used with nominal centre frequencies of ~1 MHz (in practice the quoted frequency differs somewhat from the actual response achieved). The transducers were broadband and so contained a range of frequencies around the centre frequency.

The transducer was driven by an ultrasonic pulser receiver (UPR), which was controlled by a PC. The UPR generated a series of short duration voltage pulses. The pulses excited the piezoelectric element causing it to resonate, thus sending the required ultrasonic pulse through the medium. The element operated in pulse echo mode and so received reflections back from the oil film. Reflected pulses were digitised using a PCI digitising card in the PC. The PC performed the signal processing, and displayed results with software written in the LabVIEW (from National Instruments) environment.

The first step in the signal processing was to record a reference signal. To achieve this, the bearing surfaces were separated and the oil layer removed. A measurement of the reflection was then made from the interface between the bearing material and air. Since the reflection coefficient from this interface is close to unity then the reflected signal will be equal to the incident signal. This pulse was operated on by a Fast Fourier Transform (FFT) to produce an amplitude spectrum and a phase spectrum, which were stored as references for later use.

The bearing was then reassembled and reflected pulses captured and stored for a range of film thickness cases. Each reflected pulse was converted from the time domain to the frequency domain using an FFT.

The reflected pulse in the frequency domain contains both amplitude and phase information. The amplitude spectrum from the oil film was divided by the reference amplitude spectrum to give the reflection coefficient spectrum, $R(f)$. The phase spectrum from the oil film was subtracted from the reference phase spectrum to give the phase difference spectrum $\Phi_R(f)$.

The phase and amplitude reflection coefficient spectra can then be used in equations (23) and (22) to determine the film thickness (at each measurement frequency).

Experiments on a Static Oil Film

Initially, experiments were carried out on a static oil film that could be measured by an independent means. The purpose of these tests was to explore the form of the reflected pulse amplitude and phase changes and compare these with predictions from the analytical models.

Glass Sheets and Oil Film Apparatus

A static oil film was created by sandwiching a drop of oil between two sheets of float glass 5mm in thickness (as shown in the photograph of figure 5). The mass of the oil drop is measured using an accurate electronic balance. The oil drop is pressed into a circle between the two plates. Given the mass, density and diameter of the oil circle formed, the film thickness could be approximated (to an accuracy of 5%). This measured film thickness was then used to compare with the results from the ultrasonic technique.

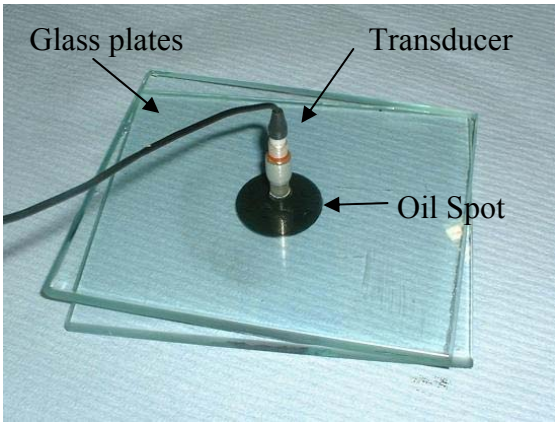

Figure 5. Oil drop sandwiched between two sheets of glass to form a model of oil film. The location of the ultrasonic element is shown.

A piezoelectric transducer was bonded directly to the upper glass sheet using a cyanoacrylate adhesive. A reference pulse (from the upper glass sheet alone) and a series of reflected pulses from different thickness oil films were recorded. The oil film thickness was varied by changing the quantity of oil used or by pressing the glass sheets together. In practice it was found that oil film thicknesses in the range 3 μm to 30 μm could be obtained in this way. Thinner oil films could not be achieved without direct contact occurring between the glass sheets at some places. Thicker oil films tended to be harder to maintain constant with time as the plates start to drift.

Results for Static Oil Film

Figure 6 shows the time domain plot of the reflected pulses from a series of oil films. A reference pulse reflected from a glass air interface is compared with subsequent pulses reflected from varying oil film thicknesses. The presence of the oil film has two effects; firstly the amplitude of the wave is reduced (as some of the wave is transmitted through the film) and secondly the phase of the reflected signal is changed as shown, for example, by a shift in lateral position of the first peak.

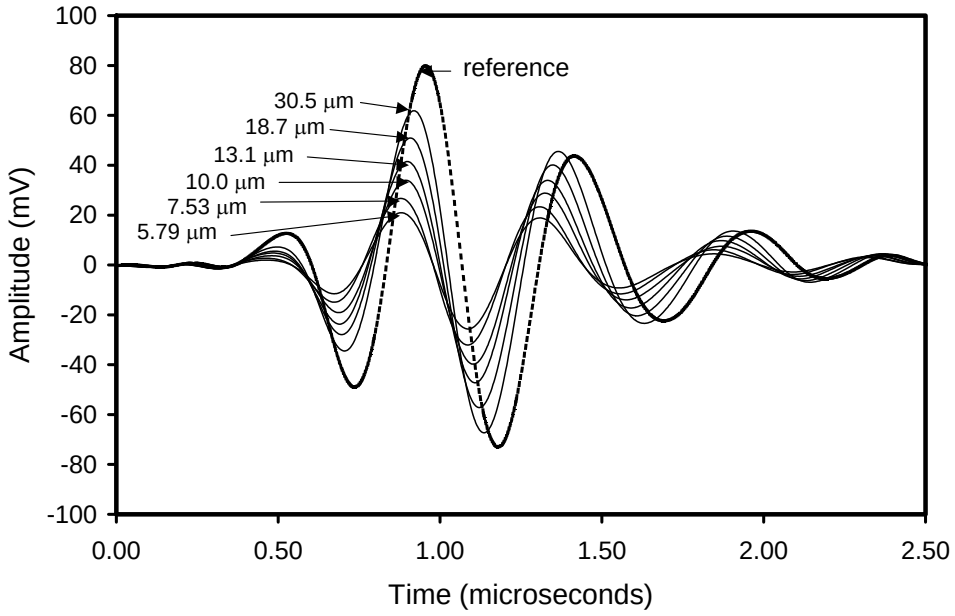

Figure 6. Reflected pulse from static oil films (between glass plates). As the oil film thickness increases the amplitude of the pulse reduces and the phase shift increases.

The time-domain signals of figure 6 were converted to the frequency domain using an FFT to obtain the amplitude and phase spectra. Firstly the amplitude spectra (shown in figure 7) were used to obtain the film thickness.

Each amplitude spectrum was divided by the reference spectrum to give the reflection coefficient (figure 8). The amplitude FFT has been over plotted (using an arbitrary vertical scale) to show the region of useful energy. Where the transducer has useful energy (from around 1.25 to 2.75 MHz) smooth frequency dependent reflection coefficient curves are obtained. Erroneous results can be noticed outside this frequency bandwidth because the signal to noise ratio is low.

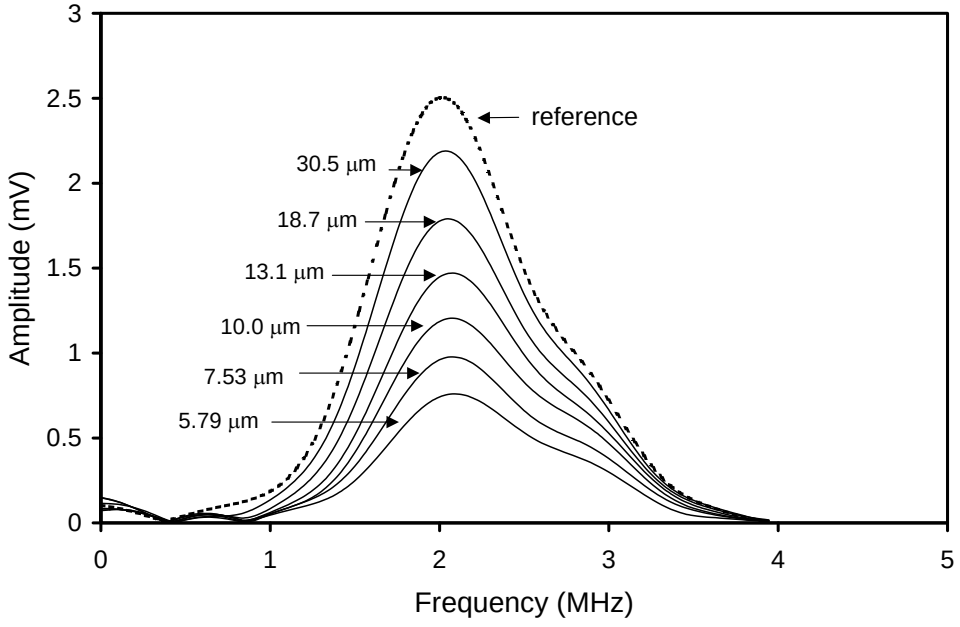

Figure 7. Amplitude spectra of reflected pulses from a series of static oil films and the reference pulse which is equivalent to the incident signal.

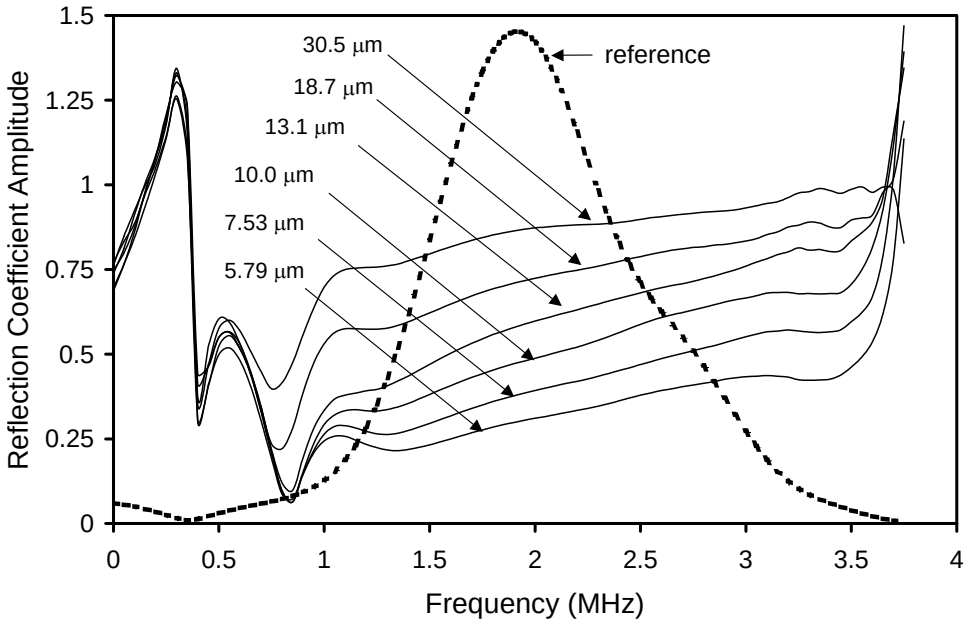

Figure 8. Amplitude reflection coefficient spectra of reflected pulse from a series of static oil films**.** The reference pulse spectrum is also shown (dotted line), with arbitrary vertical scale, to demonstrate the bandwidth of the transducer.

Equation (24) was then used to calculate the oil film thickness for each of the frequency data points of figure 8. The resulting film thickness variation with frequency is shown as figure 9. Clearly film thickness should not change with frequency; therefore within the frequency bandwidth the film thickness plots should be horizontal. This is the case and demonstrates that the frequency dependent spring model (equation 24) is an appropriate model for interpreting the data.

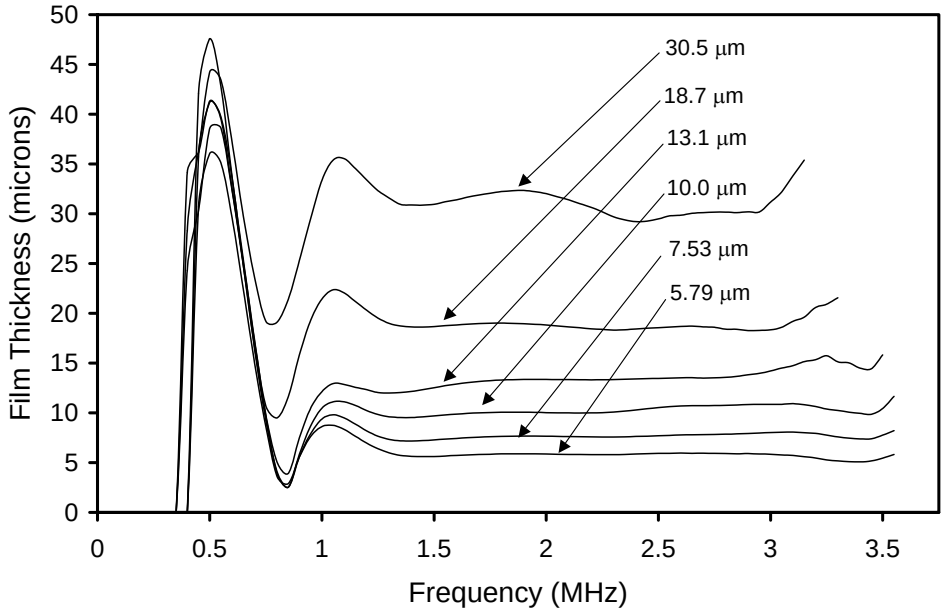

Figure 9. Oil film thickness deduced from amplitude reflection coefficient measurements variation with the measurement frequency.

The phase component of the reflected pulse is now examined. The FFT of figure 6 was used to obtain the phase spectra. These are shown as figure 10. The saw-tooth nature of the phase plots is due to the fact that phase changes continually with frequency, but can only have a value between 0 and -2π radians.

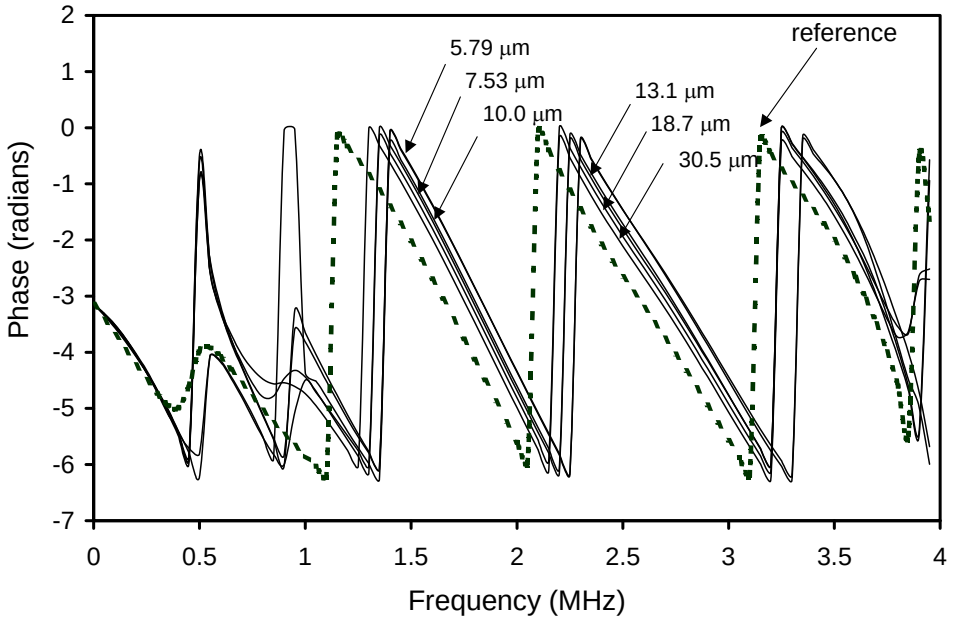

Figure 10. Phase spectra of reflected pulses from a series of static oil films and the reference pulse which is equivalent to the incident signal.

The phase shift of the reflected pulse (from the incident pulse) was calculated by subtracting the phase of the reference from the phase of each of the oil film pulses. The result is shown in figure 11.

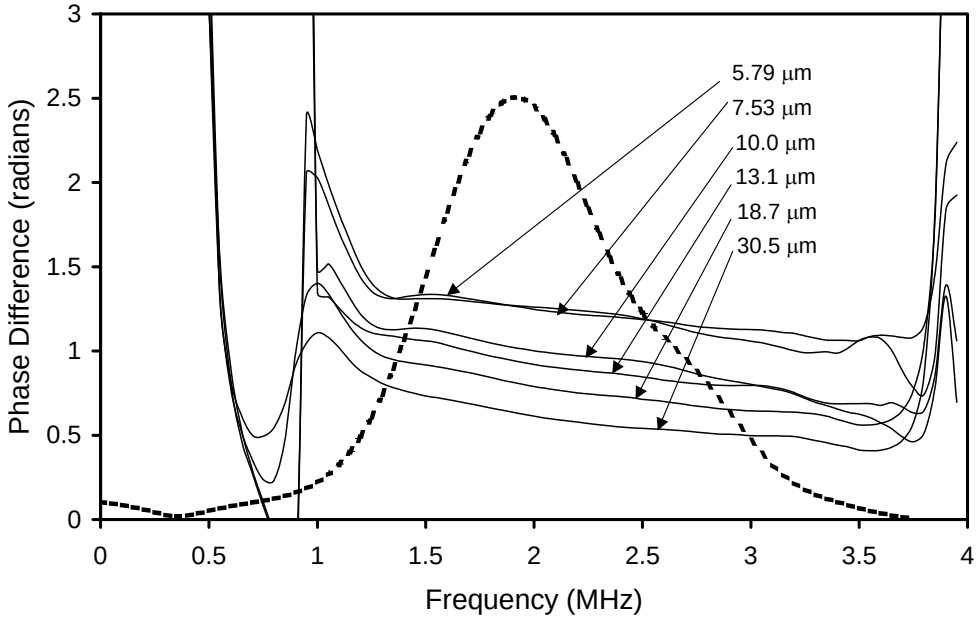

Figure 11. Phase difference spectra of reflected pulses from static oil films. The reference pulse spectrum is also shown (dotted line), with arbitrary vertical scale, to demonstrate the bandwidth of the transducer

The oil film thickness was obtained from the phase shift by using equation (25). The variation with frequency is shown in figure 12. Again, the data within the transducer frequency bandwidth is shown to be largely independent of measurement frequency.

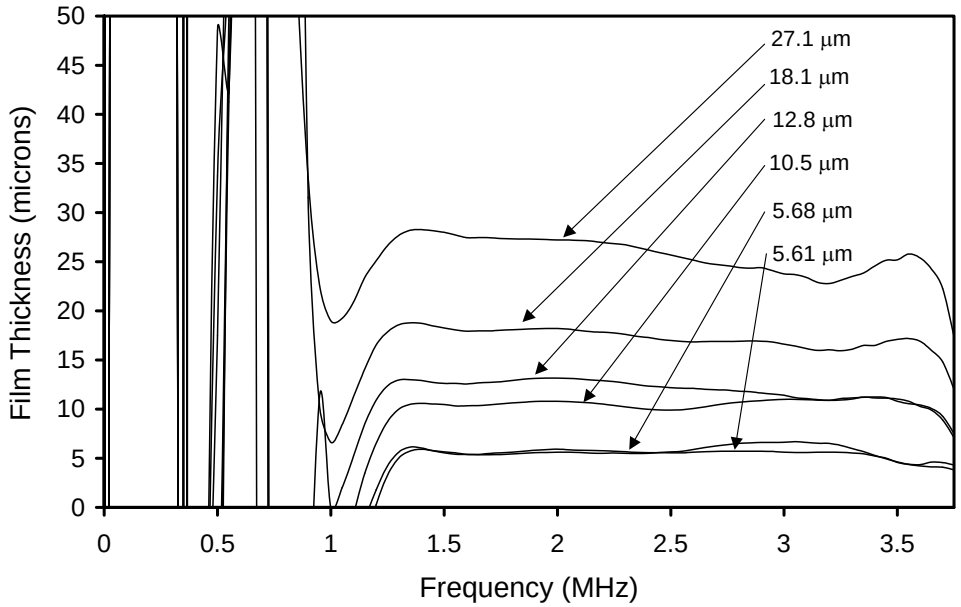

Figure 12. Oil film thickness deduced from phase shift measurements variation with the measurement frequency.

The film thicknesses determined by both amplitude and phase methods, were averaged over the useful energy region. Figure 13 shows the measured film thickness from both methods compared with the direct optical measurement method from the oil

film diameter. There is good agreement between the three methods (and within the accuracy of the method for optically determining the oil film). The scatter in the results is probably due to the waviness in the glass and the fact that the plates may not have been exactly parallel.

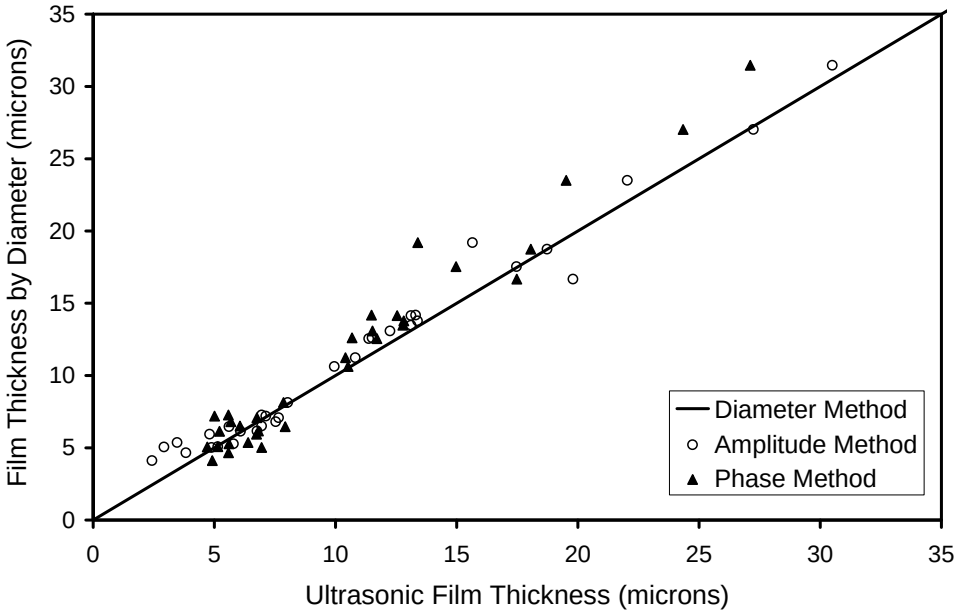

Figure 13. Comparison of amplitude and phase methods of film thickness measurement with thickness determined optically from the diameter of the spread oil spot.

It can be seen that the phase method under estimates the oil thickness at higher values. Examination of equations (22) and (23) show, that (for identical materials either side of the interface), the amplitude and phase thickness depend on material properties and frequency in the same way. Therefore, this discrepancy must be due to some inaccuracy in the phase method, which is less significant in the amplitude method. Due to the presence of a tangent term in equation (23), errors in the phase difference are amplified, as the phase difference tends to zero (i.e. as the film thickness tends to infinity). A 2% error in phase measurement would be sufficient to cause the discrepancies observed in this data at the thicker measured films.

Experiments on a Hydrodynamic Film

To compare the two methods of measurement further for application in real dynamic lubrication cases, tests were performed on a hydrodynamic journal bearing apparatus. The same approach was adopted, the reflected pulse was recorded and used to obtain reflection coefficient and phase data.

Journal Bearing Apparatus

Figure 14 shows a schematic diagram of the journal bearing apparatus and the transducer location. A steel shaft was supported on two rolling bearings and was driven by a variable speed electric motor. A brass bush (length 37.5 mm, diameter 75 mm, and radial clearance 25 μm) was fitted inside an arm that was hydraulically loaded onto the shaft. Lubricant (Shell Turbo T68) was supplied through a feeder hole at the top of the bearing. In practice it was found that a small positive pressure,

provided by a peristaltic pump, was necessary to maintain lubrication for all bearing operating conditions.

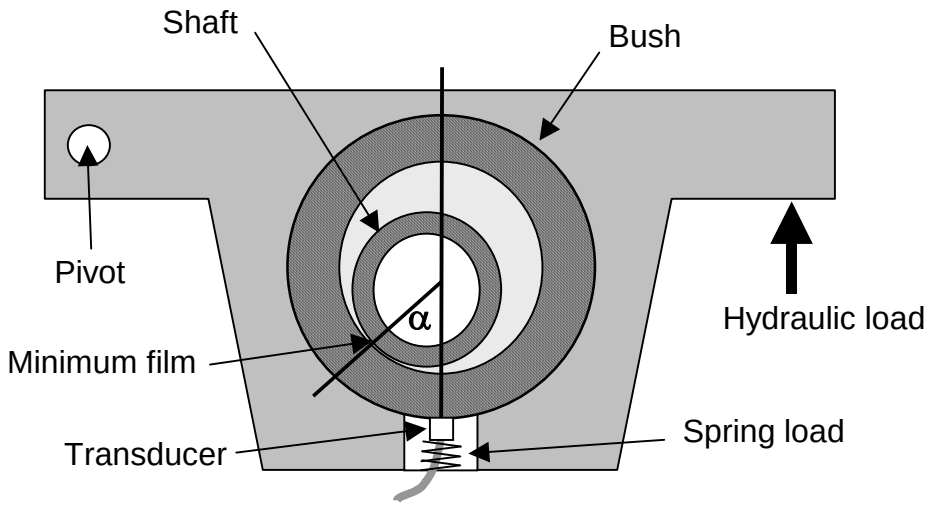

Figure 14. Schematic diagram of the journal bearing apparatus and transducer assembly.

A hole was through drilled in the loading arm to give access to the bush outer surface. A 1.1 MHz planar transducer was spring loaded onto the bush as shown. A water based ultrasonic gel was used to couple the transducer to the bush. The transducer was connected to the ultrasonic pulser-receiver and signal processing system was identical to that discribed for the glass disc tests. The transducer in its usual position is located at the maximum load point on the bearing. A K-type thermocouple was used to measure the outlet temperature of the oil as it exited the bearing. The oil temperature measurement was used to adjust the lubricant viscosity for theoretical calculations of film thickness.

Results for a Hydrodynamic Oil Film

Equations (24) and (25) were used to determine the oil film thickness from both amplitude and phase measurements. In the tests these relationships were coded into the Labview control software to provide a real time measurement of the oil film thickness by both methods. The processing time takes typically 0.1s (to download the reflected pulse, FFT, and determine the film thickness). Figures 15 and 16 show the reflection coefficient and phase difference for a series of oil films generated by changing the bearing speed at constant load.

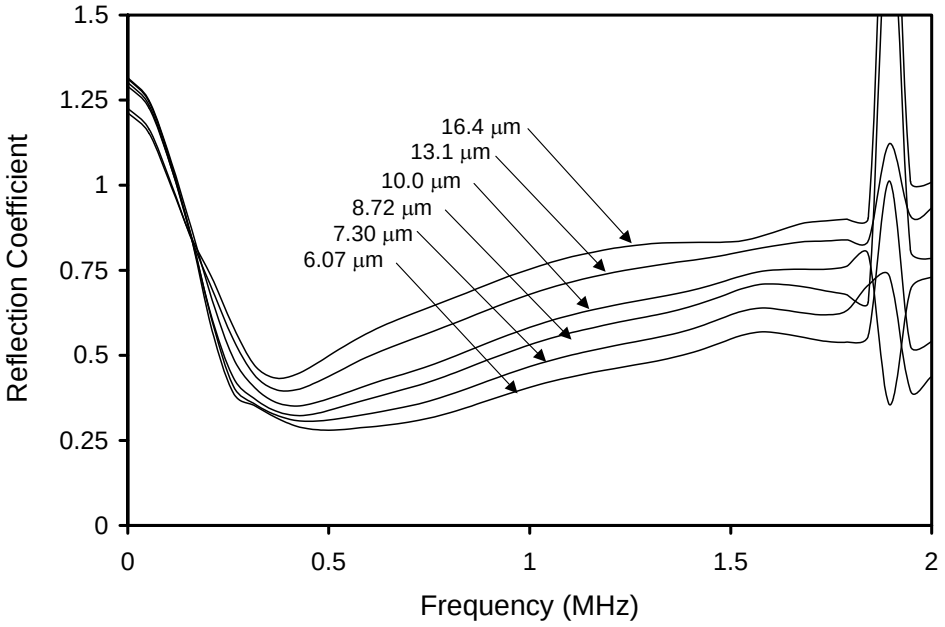

Figure 15. Reflection coefficient spectra of pulses reflected from a series of journal bearing oil films generated by varying the bearing speed at constant load.

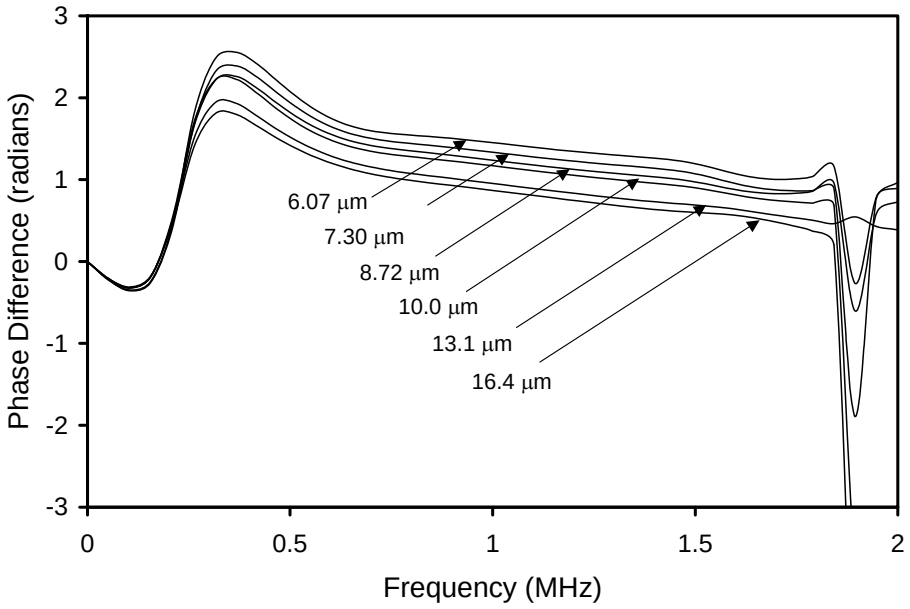

Figure 16. Phase difference spectra of pulses reflected from a series of journal bearing oil films generated by varying the bearing speed at constant load.

In Figure 17, results for both methods (amplitude and phase) are compared. The results represent film thickness measured for many repeated tests at various bearing rotational speeds. Prediction by phase method is very slightly lower but overall there is a clear overlapping of results indicating a good agreement.

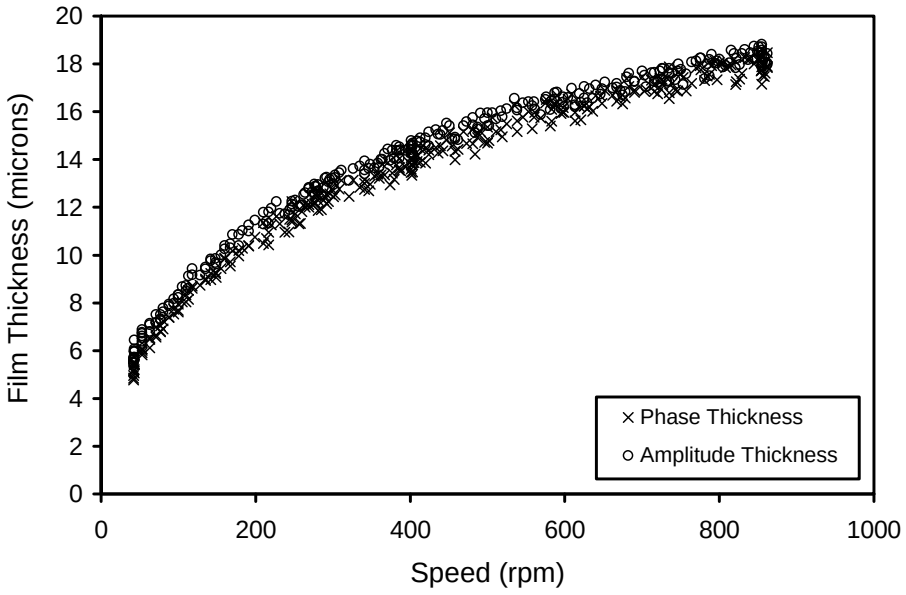

Figure 17. Oil film thickness measured by amplitude and phase based methods for a range of journal rotational speeds.

The viscosity of the oil was determined at the measured oil temperature for each data point. This was used, along with the load and speed to determine the Sommerfeld number, S according to:

$$S = \eta\omega \frac{LD}{W}\left(\frac{R}{c}\right)^2 \tag{27}$$

where η is the oil viscosity, ω is the rotational speed, L is the bearing length, D and R are the bearing diameter and radius, c is the bearing radial clearance, and W is the applied load.

Figure 18 shows the data of figure 17 re-plotted as Sommerfeld number plotted against the measured film thickness ratio, h/c. The theoretical solution of Raimondi and Boyd [17] has been used to predict the film thickness in this bearing. It should be noted that the oil film thickness measured here is at the maximum load point (i.e. directly under the applied load), labelled h_v on the figure and not the minimum film thickness, h_{min}. The solution of Raimondi and Boyd has been adapted to give the film thickness at this location and not the more commonly presented minimum film thickness.

The experimental values are lower than the theoretical values in Figure 18. This may be due the temperature used in calculating the viscosity. The temperature was taken from the oil leaking from the bottom of the journal. At this location the oil is possibly cooler than that in the film; the actual measured film could be at a higher temperature and therefore a little thinner. The in accuracy in temperature measurement is expected to be larger in the higher speed region where temperature of the oil has increased and the difference with the surrounding temperature is more. Hence, the experimental prediction has shown a greater deviation from the theoretical for higher speed values as observed in Figure 18. Another possible contributing factor is a misalignment in the journal bearing. The full load carrying capacity will only be achieved for perfect alignment between the shaft and bush.

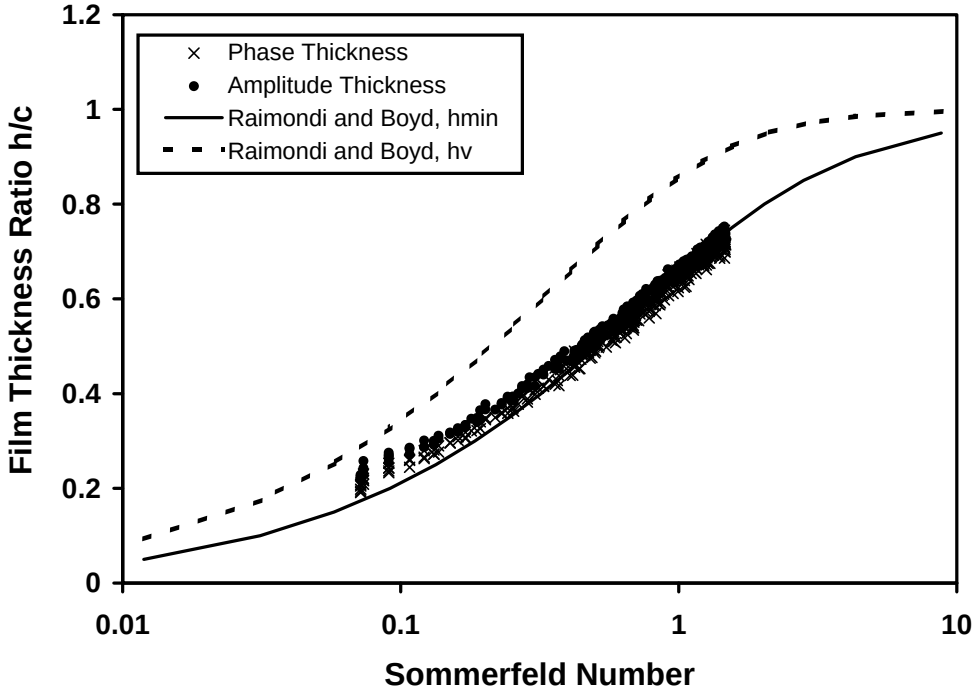

Figure 18. Experimental amplitude and phase film thickness results plotted as against film thickness ratio against Sommerfeld number. The theoretical analysis of Raimondi & Boyd [17] is over-plotted.

Incorporation of Oil Film Mass and Damping Terms

The model presented in theoretical section of this paper includes stiffness terms only. The oil film may not behave as simply as a collection of springs, it is important to determine whether the mass and visco-elastic damping terms could also be significant. A proposed spring-mass-damper model of the interface is shown figure 19.

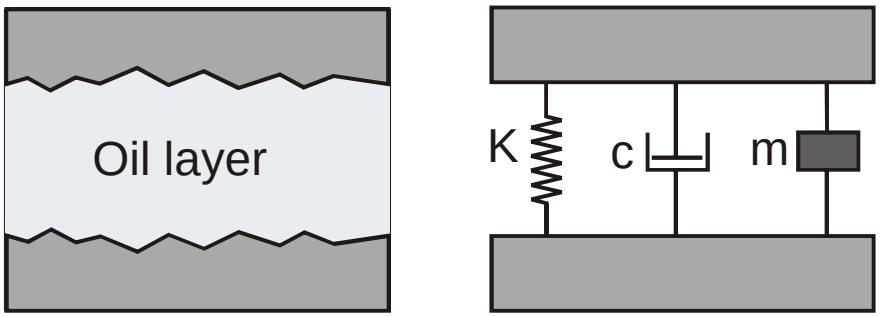

Figure 19. Schematic diagram showing a) interface and b) spring-mass-damper model of lubricant film response to ultrasound.

If the oil layer is modelled in this way, then equations 13 and 14 no longer hold. Instead the equation of motion of the layer is used. Baik and Thompson [18] developed a model for reflection from a dry contact (an interface consisting of asperity contacts and air gaps) that can also be used for a liquid layer, by using

appropriate layer properties. Their model incorporates stiffness and mass (without the damping terms). The equations of motion then become:

$$\sigma_1(0) = K(u_2(h) - u_1(0)) - \frac{m\omega^2}{4}(u_2(h) + u_1(0)) \tag{28}$$

$$\sigma_1(0) = K(u_2(h) - u_1(0)) + \frac{m\omega^2}{4}(u_2(h) + u_1(0)) \tag{29}$$

The expression for reflection coefficient as a function of mass and stiffness becomes:

$$R = \frac{(z_1 - z_2)(4K - m\omega^2) + i4\omega(z_1 z_2 - Km)}{(z_1 + z_2)(4K - m\omega^2) + i4\omega(z_1 z_2 + Km)} \tag{30}$$

where m represents the mass per unit area of the oil layer relative to the surround media:

$$m = h(\rho - \rho_m) \tag{31}$$

where ρ is the density of the oil layer and ρ_m is the density of the material either side of the interface. Figure 20 compares the predictions of this model, equation (30), with that of the spring model alone, equation (20). For all but unrealistically thick lubricant films (or very high frequencies) the spring model provides identical results to the spring-mass model. The oil films found in bearings are so thin that, for ultrasonic purposes, their mass can be neglected.

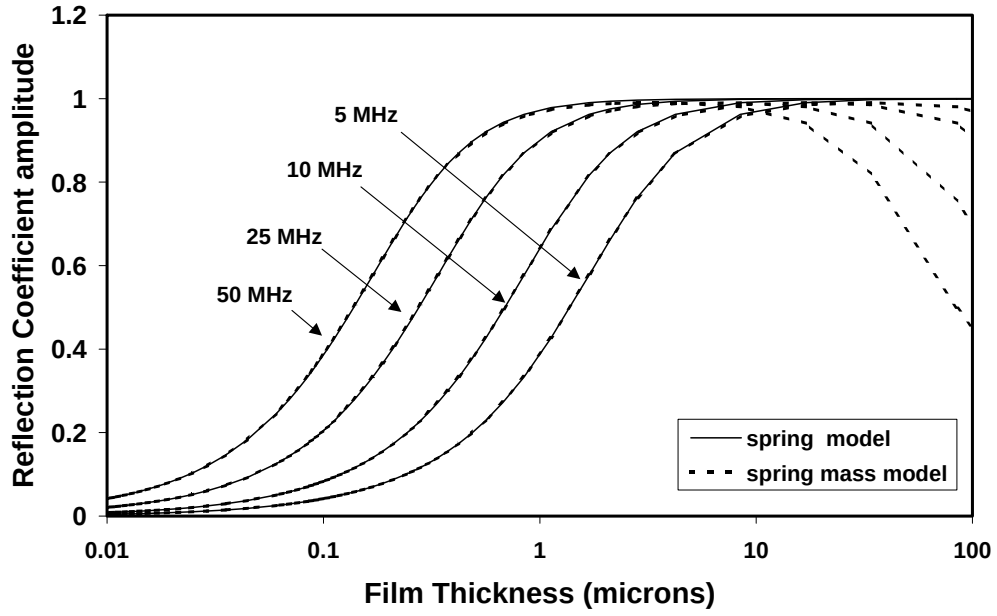

Figure 20. Plot of reflection coeficient amplitude against film thickness for the spring model and spring-mass. Both models give similar predictions unless oil films are very thick.

A similar approach was carried out by Krolikowski and Szczepek [9], incorporating stiffness and damping of an interface. Again their model was developed for the study of dry contacts. This gives a reflection coefficient according to:

$$R = \frac{(z_1 - z_2) + \frac{i\omega}{K^*}(z_1 z_2)}{(z_1 + z_2) + \frac{i\omega}{K^*}(z_1 z_2)} \tag{32}$$

Here the damping is represented by the complex modulus K^* given by

$$K^* = K(1 + i\eta) \tag{33}$$

Where η is the loss factor (also known as tan δ), and represents the fraction of total energy lost per cycle. It should be noted that this is not the same damping that might occur by the resistance to fluid flow if the journal were to oscillate (i.e. squeeze film damping). Instead, this damping term represents the energy dissipated within the oil as it undergoes cyclic compression and rarefaction.

The spring-mass model and spring-damper approaches outlined above have been combined using a similar approach to the spring model. For brevity the derivation is omitted here. The complete expression for reflection coefficient spring-mass-damper becomes:

$$R = \frac{(z_1 - z_2)(4K^* - m\omega^2) + i4\omega(z_1 z_2 - K^* m)}{(z_1 + z_2)(4K^* - m\omega^2) + i4\omega(z_1 z_2 + K^* m)} \tag{32}$$

It is convenient to represent the reflection coefficient as a vector on the complex plane whose length is equal to its amplitude, and positioned at an angle equal to its phase. Reflection coefficient amplitude increases from 0 to 1 as either frequency or film thickness increases from zero to infinity while reflection coefficient phase varies from zero to π/2 radians. The relationship between phase and amplitude (equation 26) can therefore be plotted as a locus on the complex plane on figure 21 (marked spring model). The resulting locus begins at the condition of zero frequency-thickness where reflection coefficient amplitude is zero and phase is π/2. The locus follows a semi-circular arc and ends at the condition of infinite frequency-thickness where reflection coefficient amplitude is 1 and phase is 0.

Damping terms can also be incorporated into the spring model and plotted in this way. In the absence of any data for the damping properties of Turbo T68, arbitrary values of the loss modulus have been used here. Values of η = 0.2, 0.5 and 1 have been selected as spanning the likely range of loss factors expected for long chain polymer behaviour. These three cases are shown on figure 21. Experimental reflection coefficients from varying film thickness and frequencies have been over plotted (shown as data points).

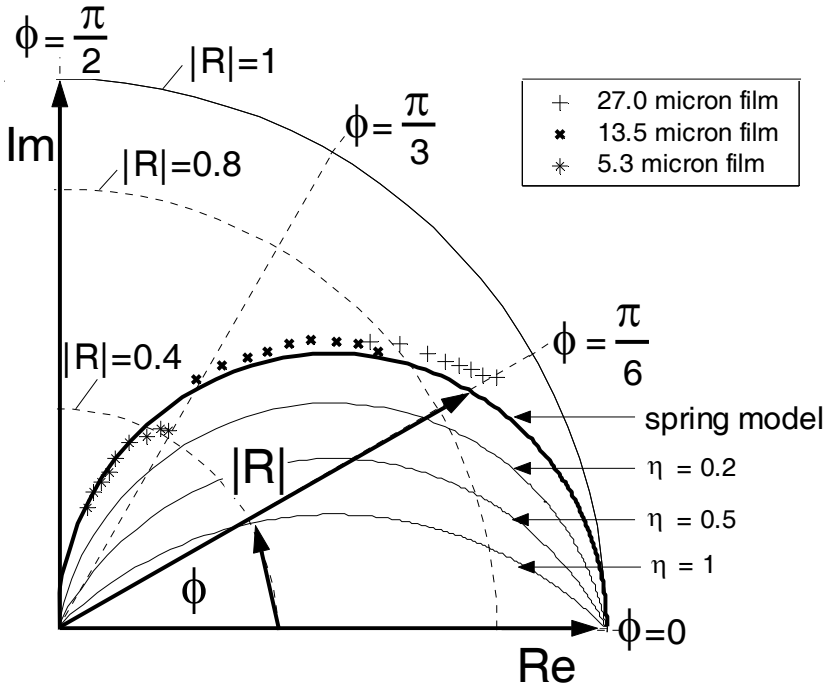

Figure 21. Complex reflection coefficient plotted on an Argand diagram. The spring model is compared to a spring-damper model for three loss factors. The experimental data is the reflection coefficient variation with frequency for three film thicknesses.

There is good agreement between the experimental results and the reflection coefficient locus for zero damping. This means that, once again, the spring model incorporating stiffness alone provides a satisfactory representation for the ultrasonic response of a thin oil layer. The damping properties of the oil are negligible, due again, to the small volume of liquid in the film that can cause only minimal energy dissipation.

Reference Signal Deduction From Phase and Amplitude Measurements

There is one potentially very useful outcome of simultaneous measurements of amplitude and phase. This is that it can be used to remove the need for a reference incident signal [15].

If the phase and magnitude of a reflected pulse are measured simultaneously over a range of film thickness values and frequencies (i.e. there is no mass and damping effects) then the simple relationship between the two (equation (26) can be used to negate the requirement for a reference.

As detailed above, the amplitude of the reflection coefficient is given by the ratio of the amplitudes of the wave reflected from a film A, to that when the wave is completely reflected A_0, (i.e. it is compared to the wave reflected from a material/air interface).

$$|R| = \frac{A}{A_0} \tag{35}$$

Similarly, the phase of the reflection coefficient is given by the phase of the wave reflected from a film ϕ, minus the phase of the completely reflected wave ϕ_0.

$$\Phi_R = \phi - \phi_0 \tag{36}$$

Equations 33 and 34 can be substituted into 24 to give

$$A = A_0 \cos(\phi - \phi_0) \tag{37}$$

This relationship is the basis of the method for deducing the reference signal (i.e. the reference amplitude and phase A_0 and ϕ_0). In practical terms, the reflected amplitude and phase A and ϕ are measured simultaneously as the oil film thickness varies. For a given frequency, the data pairs are plotted against each other and equation 37 is fitted to the data. A least mean squared (LMS) algorithm is suitable for this. The fitting of this curve gives the two constants A_0 and ϕ_0 at that frequency.

This approach was applied to the data from the glass plate tests. The amplitude and phase at the centre frequency of the waves reflected from the films are shown in figure 22 along with the fitted LMS curve.

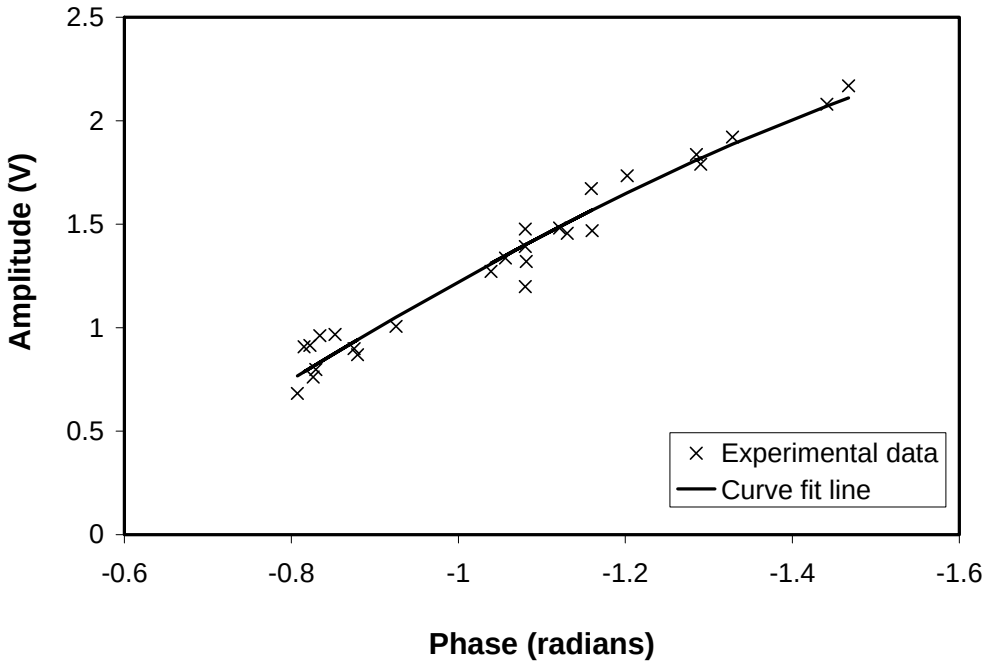

Figure 22. Plot of amplitude against phase at the centre frequency of the wave reflected from the oil film, with LMS curve-fit line.

The resulting reference amplitude and phase deduced are displayed along side values found directly by experiment in table 1. There is excellent agreement between the measured and deduced reference values. It should be noted that the error values are not simply the error in the LMS (reference free) prediction; they are also generated by inaccuracies in the direct experimental values.

	Experimental value	LMS Prediction	Percentage error
A_0 (V)	2.496	2.5702	2.89
ϕ_0 (radians)	1.0492	1.0668	1.65

Table 1. Comparison of reference amplitude and phase found experimentally with those found using the LMS prediction.

The proximity of the predicted values to those found experimentally (i.e. a low error) will naturally depend on the amount of data available for the curve fitting operation. This in turn will depend on the range of film thickness available for measurement. The input data used here was from films in the range 5μm to 27μm corresponding to a reflection coefficient range of 0.274 to 0.869. The relationship between the available data range and the accuracy of the predicted reference remains to be determined.

Discussion

Both the amplitude and phase methods compared here show a satisfactory means for measurement of oil film thickness. In terms of the ease and speed of measurement there is little to choose between the two approaches. Both the amplitude and phase respond in the same physical way to an embedded oil film between metal surfaces.

The measurements presented here compare closely with independent theoretical and experimental assessments of oil film thickness. The accuracy of the results presented is at least as good as the theoretical and empirical comparatives. However, ultrasonic amplitude measurements are subject to error associated with signal noise (especially in an electrically noisy industrial environment). It is possible that phase measurements are less prone to these kinds of error. This has yet to be explored.

Another feature of piezoelectric ultrasonic measurements is that the transducers are temperature sensitive. A rise in the ambient temperature causes an increase or decrease (depending on the transducer) in the amplitude of launched ultrasonic pulse. Whilst this effect is not significant for atmospheric temperature changes, for bearings that may run up to 150°C or so, there may be a significant signal reduction/increase. The extent of which depends on the transducer and the bonding layer coupling the transducer. This manifests itself as an apparent fall/rise in the film thickness, unless a new reference is recorded at the elevated temperature. In practice this effect has to be compensated for. It had been hoped that the phase change of an output pulse from a piezo material would not be sensitive to temperature. An experiment performed as part of this work but omitted for brevity (using a transducer heated in oven), showed that this is not the case. The phase difference is just as sensitive as the amplitude to changes in temperature. There is thus no advantage to using the phase method in this respect.

The simple relationship between amplitude and phase, equation (26) is only true when oil film mass and damping terms are neglected. When mass and damping is included the relationship changes and measurements of reflection coefficient could be used to determine the actual damping of the oil film (in terms of the loss factor) by simultaneous solution of the magnitude and phase components in equation (32). It happens that the quantity of oil in the film is so little that its mass and damping effects are negligible.

One potentially very useful outcome of this investigation into simultaneous phase and reflection measurements has been the development of the reference method. The

results showing that the reference signal can be deduced, with a high degree of accuracy, from the history of measured pairs of amplitude and phase. This means that the bearing does not need to be disassembled to provide an air reference, and further the measurements can be self-calibrating. This method will only work if, during normal operation, the bearing displays a range of film thicknesses and enough discrete reflection data can be obtained. The online implementation of this technique and the assessment of its limitations will be the subject of further study.

Conclusions

It has been shown that the phase of reflection coefficient can be used to determine the oil film thickness in the same way as the amplitude based methods. Both methods have been validated using a simple static oil film apparatus; and good agreement has been achieved with independent means of measurement.

The application to film measurement in a hydrodynamic journal bearing has demonstrated the usefulness of both phase and amplitude methods for analysis of real lubrication cases. The results of the journal bearing study agree well with theoretical numerical solutions.

A simple relationship between reflection coefficient amplitude and phase has been derived. This is plotted as a locus on the complex plane alongside measured film thickness results. The model has been recast to incorporate mass and damping terms. Comparisons with the more complex model demonstrate that both mass and damping terms are have a minor effect for practical lubrication cases and can be neglected.

The implementation and validation of the reference technique has great practical benefits. Experimental procedures will be simplified, and film thickness in previously impossible situations will become measurable (where parts cannot be dismantled).

Acknowledgments

The authors are grateful for to Dr Jie Zhang, University of Bristol for his help in some of the modelling aspects of this work.

References

[1] Astridge, D.G. and Longfield, M.D., (1967), Capacitance Measurement and Oil Film Thickness in a Large Radius Disc and Ring Machine, Proc. Instn. Mech, Engrs., Vol. 182, No. 3N, pp. 89-96.

[2] Chu, P. S. Y., and Cameron, A. (1967), Flow of electric current through lubricated contacts, *ASLE Transactions,* Vol 10, pp.226-234.

[3] El-Sisi, S.I. and Shawki, G.S.A., (1960), Measurement of Oil-Film Thickness Between Disks by Elecrical Conductivity, Trans. ASME J. Basic Engng., Vol. 82D, p.12.

[4] Cameron, A. and Gohar, R., (1966), Theoretical and Experimental Studies of the Oil Film in Lubricated Point Contact, Proc. Roy. Soc. Lond., Vol. 291A, pp. 520-536.

[5] Richardson, D.A. and Borman, G.L., (1991), Using Fibre Optics and Laser Fluorescence for Measuring Thin Oil Films with Applications to Engines, SAE Paper 912388.

[6] Tattersall, H.G., (1973), the ultrasonic pulse-echo technique as applied to adhesion testing, *J.Appl. Phys.D.*, Vol. 6, pp. 819-832.

[7] Pialucha, T., and Cawley, P (1994), The detection of embedded layers using normal incidence ultrasound, Ultrasonics, Vol 32, pp. 431-440, 1994.

[8] Nagy, P.B., (1992), Ultrasonic classification of imperfect interfaces, Journal of Nondestructive Evaluation, Vol. 11, pp. 27-139.

[9] Haines, N. F., The theory of sound transmission and reflection at contacting surfaces, Report RD/B/N4744, CEGB Research Division, Berkeley Nuclear Laboratories, 1980.

[10] Baltazar, A., Rokhlin, S. I., and Pecorari, C., (2002), On the relationship between ultrasonic and micromechanical properties of contacting rough surfaces. *J.Mech. Phys.* Vol. 50, pp. 1397-1416.

[11] Kendall, K. and Tabor, D., (1971), An ultrasonic study of the area of contact between stationary and sliding surfaces, *Proc. R. Soc. Lond.* A, Vol. 323, pp. 321-340.

[12] Krolikowski, J. and Szczepek J., (1991), Prediction of contact parameters using ultrasonic method, *Wear*, Vol. 148, pp. 181-195.

[13] Drinkwater, B.W., Dwyer-Joyce, R. S., and Cawley, P. (1996), A study of interaction between ultrasound and a partially contacting solid-solid interface, *Proc. R. Soc. Lond*. Vol.452, pp 2613-2628.

[14] Krolikowski, J. and J. Szczepek, (1992), Phase shift of the reflection coefficient of ultrasonic waves in the study of the contact interface, *Wear, 157*, 51-64.

[15] Offterdinger, K. and Waschkies, E., (2003), Temperature dependence of the ultrasonic transmission through electrical resistance heating imperfect metal-metal interfaces, NDT&E International. Vol. 37, pp. 361-371.

[16] Dwyer-Joyce, R.S., Drinkwater, B.W., and Donohoe, C.J., (2002), "The Measurement of Lubricant Film Thickness using Ultrasound", Proceedings of the Royal Society Series A, Vol. 459, pp 957-976.

[17] Dwyer-Joyce, R.S., Reddyhoff, T., and Drinkwater, B., (2004), 'Operating Limits for Acoustic Measurement of Rolling Bearing Oil Film Thickness', STLE Tribology Transactions, pp. 366-375, Vol. 47, No. 3.

[18] Dwyer-Joyce, R.S., Harper, P., and Drinkwater, B., (2004), 'A Method for the Measurement of Hydrodynamic Oil Films Using Ultrasonic Reflection', Tribology Letters, Vol. 17, pp. 337-348.

[19] Harper, P., Dwyer-Joyce, R.S., Sjödin, U., and Olofsson, O, (2005), Evaluation of an Ultrasonic Method for Measurement of Oil Film Thickness in a Hydraulic Motor Piston Ring, in press Proceedings of the 31st Leeds-Lyon Symposium on Tribology, Elsevier.

[20] Dwyer-Joyce, R.S., Harper, P., Pritchard, J, and Drinkwater, B., (2005), 'Investigation into Film Formation in a Hydro-Electric Power Station Thrust Bearing', in press Tribology International.

[21] Raimondi, A.A. and Boyd, J., (1958), A solution for the finite journal bearing and its application to analysis and design -I -II, -III, ASLE Trans., Vol. 1, No. 1, I- pp. 159-174, II - pp. 175-193, III - pp. 194-209.

[22] Baik, J-M., and Thompson, R.B., Ultrasonic scattering from imperfect interfaces: a quasi static model, Journal of Nondestructive Evaluation, Vol. 4 , pp. 177-196.